Sensors and Actuators A 179 (2012) 178–184

Contents lists available at SciVerse ScienceDirect

Sensors and Actuators A: Physical

journal homepage: www.elsevier.com/locate/sna

Design and characterization of miniature piezoelectric generators with low resonant frequency

Ziping Cao [a,b], Jinya Zhang [a,b,*], Hiroki Kuwano [b]

[a] Institute of Communication Technology, Nanjing University of Posts and Communications, Nanjing 210003, China
[b] Department of Nanomechanics, Graduate School of Engineering, Tohoku University, Sendai 980-8579, Japan

ARTICLE INFO

Article history:
Received 25 October 2011
Received in revised form 16 January 2012
Accepted 20 February 2012
Available online 21 March 2012

Keywords:
Vibration energy harvesting
Piezoelectric generators
AlN
Piezoelectric thin films

ABSTRACT

In this study, both materials selection and device configuration design were considered for developing miniature piezoelectric generators with low resonant frequency. Instead of single crystal Si, stainless steel (SUS) was chosen as the substrate of AlN thin films owing to its higher fracture toughness, which made it possible that millimeter-scale generators had resonant frequency of less than 100 Hz. The device configuration including the aspect ratio (the length of the cantilever to the width of the cantilever) and the thickness ratio (the substrate layer to the AlN film layer) were analyzed for optimizing transverse electromechanical coupling coefficient of generators. Using AlN thin films deposited on stainless steel, millimeter-scale generators were fabricated and their vibration energy harvesting performance was characterized. Output power and resonant frequency of the devices are, respectively, 5.130 μW and 69.8 Hz when they were vibrated at 1 g acceleration and connected with 0.7 MΩ electric loading.

© 2012 Elsevier B.V. All rights reserved.

1. Introduction

Ubiquitous networks of wireless sensors have the potential to significantly benefit modern society and create large commercial opportunities. Their network nodes are generally designed to run on batteries, but the replacement of depleted batteries becomes laborious and even impractical as wireless sensors increase in huge number. Therefore, alternative methods for powering these devices are needed. Extracting energy from environmental sources is attractive as inexhaustible replacements for batteries, and has recently received increasing interest within both academic community and industry. There are several power-generating options from environmental sources including vibration, light, temperature gradient and wind, and each type has its benefits for certain applications. Mechanical vibration is one of the most widespread energies in environment which commonly goes unused. Three kinds of generators including electromagnetic, electrostatic and piezoelectric have been suggested for vibration energy harvesting. Piezoelectric generators have taken the most attention due to their simple configuration and high energy converting efficiency [1–4].

Piezoelectric generators convert mechanical energy into electric energy: electric charges are generated when piezoelectric materials are deformed due to a vibration or a force. In the practical application, a good piezoelectric generator is required to hold not only suitably low resonant frequency to match the frequency of vibration sources (usually below 200 Hz), but also high enough output power. These two requirements are easily met for piezoelectric generators with large size [3,4], however, they become challenging for miniature generators with millimeter or smaller size [5–9]. This is because that with the decrease of the device size, the resonant frequency rapidly increases and simultaneously the output power of generators gradually decreases.

In this study, for developing practicable piezoelectric generators with millimeter size, we firstly analyzed what kinds of materials should be adopted for ensuring that the devices with the cantilever structure hold low resonant frequency and high mechanical safety. For further improving the energy conversion efficiency, we calculationally optimized the device configuration including the aspect ratio (the length of the cantilever to the width of the cantilever) and the thickness ratio (the substrate layer to the AlN piezoelectric layer). Finally, AlN thin films deposited on stainless steel (SUS) substrates were prepared with an electron cyclotron resonance (ECR) system, and they were further used to fabricate millimeter-scale piezoelectric generators.

2. Material selection of miniature piezoelectric generators

When a piezoelectric generator works, output power is dependent upon both the converted mechanical energy and the lost energy. The electromechanical coupling coefficient K directly

* Corresponding author at: Department of Nanomechanics, Graduate School of Engineering, Tohoku University, Sendai 980-8579, Japan. Tel.: +81 22 795 4771; fax: +81 22 795 4771.
E-mail address: zhang@nanosys.mech.tohoku.ac.jp (J. Zhang).

0924-4247/$ – see front matter © 2012 Elsevier B.V. All rights reserved.
doi:10.1016/j.sna.2012.02.026

quantifies the ability of mechanical–electric energy conversion. The mechanical quality factor Q is related to the mechanical loss, and the dielectric loss $\tan\delta$ is involved into the electric loss (a part of electric energy is dissipated by transforming it into thermal energy). Therefore, K, Q and $\tan\delta$ can be considered as three critical parameters for designing a piezoelectric generator [2]. For miniaturizing the volume of piezoelectric generators, the piezoelectric element in these devices generally takes the form of thin film. Therefore, the material selection is mainly involved into which kinds of substrate and piezoelectric thin film are adopted. The selected materials should ensure that generators hold high Q, K and $\tan\delta$. In addition, because generators continuously work in a vibration environment, the selected materials should have high enough mechanical strength.

2.1. Selection of substrates

A miniature piezoelectric generator is mainly fabricated from the structure of piezoelectric thin film/substrate. The volume of the substrate is much larger than that of the piezoelectric thin film, so Q and mechanical strength of the device are almost determined by the substrate, and to some extent the K value of the device is also affected by the substrate. A stiff substrate is preferred for obtaining high Q and K [10], which means that the substrate needs to have both high elastic modulus and high fracture strength (or yield strength). By considering that the resonant frequency of piezoelectric generators should be low to match the frequency of most vibration sources, the thickness of the substrate should be made to be very thin. Therefore, the vibrational operation environment requires that the substrate should also possess high enough fracture toughness.

In generally, single crystal Si is used as substrates of piezoelectric thin films, because of its easy process, high temperature chemical stability and not high cost. Due to high elastic modulus and fracture strength of Si substrates, piezoelectric thin films deposited on them can be fabricated into generators with high Q and K. However, it should be noted that Si is very brittle and the fracture toughness of (1 0 0) oriented single crystal Si is only 0.95 MPa $m^{1/2}$, which incurs that the resonant frequency of miniature generators cannot be designed to be low enough through the way of thinning the thickness of the substrate. As alternatives, some metals such as SUS and Titanium may be good choices due to their high elastic modulus, yield strength and fracture toughness. Table 1 lists mechanical properties of (0 0 1) oriented single crystal Si and some metals. Among them, it seems that SUS is desirable for being used as substrates of piezoelectric thin films for fabricating miniature generators with low resonant frequency if the compatibility with micromachining technologies is not required. Ti is desirable for being used as the substrate if the micromachining compatibility is considered. Recently, the technology of the metal anisotropic reactive ion etching with oxidation process was successfully developed for fabricating arbitrarily high-aspect-ratio structures from Ti substrates with various thicknesses [11,12]. The miniature structure of Cu and Ni can be made with the electroplating processing. This processing is also compatible with micromachining technologies, but relatively low yield strength of both metals implies that their stiffness is relatively low and thus Q of the fabricated structures is also relatively low. Therefore, it is not suitable to use Cu and Ni as the substrates in piezoelectric generators.

Table 1
Mechanical properties of (0 0 1) oriented single crystal Si and some metals.

Materials	Elastic modulus (GPa)	Yield strength (MPa)	Fracture toughness (MPa $m^{1/2}$)
(0 0 1) oriented Si	130	600–7700 (fracture strength)	0.95
SUS304	197	205	80
Bulk Ti	106	170	75
Bulk Cu	117	100	–
Bulk Ni	204	58	–
Bulk Al	69	15	14–28

2.2. Selection of piezoelectric thin films

For piezoelectric thin films deposited on substrates, there are two work modes: d_{33} and d_{31}. The d_{31} mode implies that the piezoelectric layer is sandwiched between top and bottom electrodes. The d_{33} mode means that a pair of interdigital electrodes is formed on the top surface of piezoelectric thin films. The piezoelectric element cannot be easy to be completely poled and only a partial volume is effectively utilized in the operation. Therefore, although electromechanical coupling coefficient of the d_{33} mode is much higher than that of d_{31} mode, output power of a d_{33} mode generator is normally poorer than that of a d_{31} generator with the similar size [13,14].

For d_{31} mode generators fabricated from piezoelectric thin films, Q is mainly determined by the substrates so the left piezoelectric parameters for selecting piezoelectric materials are k_{31} and $\tan\delta$. The selected piezoelectric materials are also expected to have high mechanical strength such as fracture strength and fracture toughness. Up to now, piezoelectric thin films which can be prepared with matured technologies include lead titanate zirconate (PZT), ZnO and AlN. Tables 2 and 3 list piezoelectric and mechanical properties of these thin films that were reported. It can be seen that PZT thin films have the highest k_{31}, so generators fabricated from them should yield highest output power. However, there are a few unsolvable problems for PZT thin films: (1) the crystallization temperature of PZT is in the range of 600–700 °C, which is not compatible with the CMOS integration; (2) exerting a high electric field for poling is necessary, which may be difficult for PZT thin films that have some defects or pinholes; (3) the performance is gradually deteriorative due to aging effect; (4) high content of lead is unhealthy to human being. For AlN and ZnO thin films, their k_{31} is lower than that of PZT to a certain degree, but they do not

Table 2
Piezoelectric properties of PZT, AlN and ZnO thin films.

Materials	Electromechanical coupling coefficient k_{31}	Dielectric loss $\tan\delta$	Others
PZT 53/47 thin films [15]	20%	0.01–0.04	• High crystallization temperature • Need poling • Aging effect
AlN thin films [16]	14%	0.003	• Low crystallization temperature • No poling • No aging effect
ZnO thin films [17,18]	<18%	0.01–0.1	• Low crystallization temperature • No poling • No aging effect

Table 3
Mechanical properties of bulk PZT, AlN and ZnO.

Materials	Elastic modulus (GPa)	Fracture strength (MPa)	Fracture toughness (MPa $m^{1/2}$)
Bulk PZT 53/47 [19–21]	50–100	97	1.0–1.1
Bulk AlN [22,23]	330	265	2.6
Bulk ZnO [24]	140–183	100–125	1.25–1.42

suffer from the mentioned problems of PZT. In comparison with AlN, ZnO may have higher k_{31}, but in general its dielectric loss is very large, which can cause a great deal of electric energy is dissipated by converting them into thermal energy. Moreover, the mechanical strength (fracture strength and fracture toughness) of ZnO is much lower than that of AlN. For these reason, in this study, AlN thin films are used to fabricate miniature piezoelectric generators.

3. Configuration design of miniature piezoelectric generators

A piezoelectric generator usually takes the form of a cantilever beam with a proof mass at the free end. One of the most important for the cantilever configuration is: the resonant frequency of a cantilever is much lower than that of most other structures such as a bridge or a diaphragm, and thus it is easier to make the vibration of the device match with the vibration in environment. A proof mass is attached at the free end of the cantilever for further lowering the resonant frequency. In this study, the design consideration of the generator configuration mainly includes two aspects: (1) the optimal aspect ratio between the length and width of the cantilever; (2) the optimal thickness ratio between the substrate and piezoelectric thin film. The total thickness of the cantilever is expected to be thin as much as possible because the resonant frequency of the device is necessarily low.

3.1. Optimization of aspect ratio between the length and width of a cantilever

In the IEEE piezoelectric standard, the boundary conditions for defining the transverse electromechanical coupling coefficient k_{31} is that in a long plate-like piezoelectric specimen all stress components are zero except the stress along the length [25]. This boundary condition requires that the length should exceed four times longer than the width of the specimen. Actually, it is known that electromechanical coupling coefficient varies for different geometric configurations of piezoelectric devices. Recent reports showed that the transverse electromechanical coupling coefficient greatly increases as the length of the plate-like sample decreases [26,27].

Fig. 1 shows the geometry of a plate-like piezoelectric specimen with the d_{31} work mode. The aspect ratio between the length and the width is defined with $G = l_1/l_2$. According to the theory of Kim et al. [26], a general formula for the transverse electromechanical coupling coefficient is below:

$$k_{31}^G = \frac{\left\{1 - g(G)(s_{12}^E/s_{11}^E)\right\} d_{z1}}{\sqrt{S_{11}^E\{\varepsilon_{zz}^T - g(G)(d_{z1}^2/s_{11}^E)\}\{1 - g(G)(s_{12}^E/s_{11}^E)^2\}}} \quad (1)$$

where

$$g(G) = \frac{1}{G}\frac{(1+\alpha_1\alpha_3)}{\sqrt{(1+\gamma)(1+\gamma-2\alpha_1\alpha_3)}}\frac{f_b}{f_a},$$

$$\alpha_1 = \sqrt{\frac{(c_{13}^E)^2}{c_{11}^E c_{33}^D}}, \quad \alpha_3 = \sqrt{\frac{(c_{13}^D)^2}{c_{11}^E c_{33}^D}}, \quad \gamma = \frac{c_{12}^E}{c_{11}^E},$$

$$\frac{f_b}{f_a} = \frac{(\Omega_1 - \sqrt{\Omega_1^2 - \Omega_2})^{1/2}}{(\Omega_1 + \sqrt{\Omega_1^2 - \Omega_2})^{1/2}},$$

$$\Omega_1 = (1+\alpha_1\alpha_3)(1+G^2) \quad \text{and} \quad \Omega_2 = 4(1-\gamma)(1+\gamma-2\alpha_1\alpha_3)G^2.$$

where $S_{i,j}^E$ is the elastic compliance under short circuit, d_{z1} is piezoelectric constant, ε_{zz}^T is the free dielectric constant along the poling direction, and $c_{i,j}^E$ and $c_{i,j}^D$ are the stiffness constants under short and open circuits, respectively. The material parameters of AlN thin films [16,28] are showed in Table 4. k_{31}^G as a function of G was calculated and then illustrated in Fig. 2. With the decrease of G, k_{31}^G continuously increases. In the range of $G = 0.4$–4, it changes rapidly. In the case of $G < 0.4$, k_{31}^G is stable and its value at $G = 0.4$ is 0.201. When $G > 4$, k_{31}^G also varies slightly, and its value at $G = 4$ is 0.151. It can be seen from Fig. 2 that $G < 0.4$ is preferable for piezoelectric specimens if high transverse electromechanical coupling coefficient is expected. In a miniature piezoelectric generator, the piezoelectric thin film deposited on the substrate is also plate-like, therefore, the relationship between the electromechanical coupling coefficient and the aspect ratio should be considered for the configuration design of the cantilever beam.

3.2. Optimization of thickness ratio between the substrate and piezoelectric layer

In a miniature piezoelectric generator with the d_{31} work mode, a piezoelectric thin film is usually supported by a substrate, and

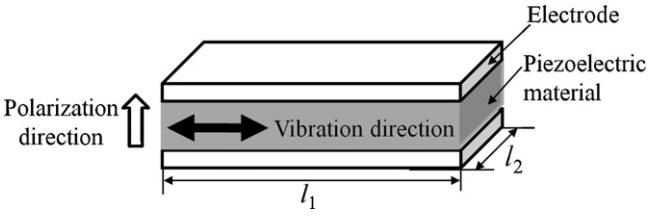

Fig. 1. Geometry of plate-like piezoelectric specimen with d_{31} mode.

Table 4
Material parameters of AlN thin films.

Elastic properties $c_{\lambda\mu}$ (N/m^2) $s_{\lambda\mu}$ (m^2/N)	Piezoelectric constant $d_{i\lambda}$ (pC/N)	Dielectric constant
$c_{11}^E = 396\times10^9$ $c_{12}^E = 137\times10^9$ $c_{13}^E = 108\times10^9$ $c_{33}^E = 373\times10^9$ $c_{11}^E = 3.0\times10^9$ $c_{12}^E = -0.9\times10^9$ $c_{12}^E = -0.9\times10^9$ $c_{33}^E = 396\times10^9$	$d_{31} = 2.65$ $d_{33} = 5.53$	$\varepsilon_{33}^T = 12.0$

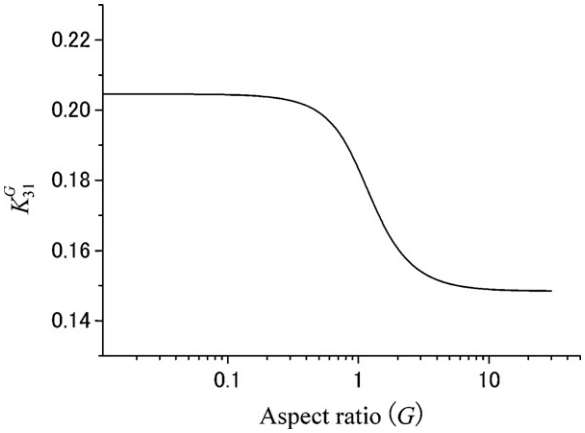

Fig. 2. Transverse electromechanical coupling coefficient as a function of the aspect ratio G in a plate-like AlN specimen.

sandwiched between a top electrode and bottom one. The volume of the substrate is generally much bigger than that of the thin film, and thus the substrate considerably constrains the motion and vibration of the piezoelectric component. As a result, the electromechanical coupling coefficient is partly suppressed by the substrate. The effective coupling factor k_{eff} of piezoelectric thin films grown on substrates is estimated with the formula [10]:

$$k_{eff}^2 = \frac{9k_{31}^2}{4}\frac{A^2B^2(1+B)^2}{[A^2B^4+2A(2B+3B^2+2B^3)+1-k_{31}^2AB(1+AB^3)](AB+1)},$$
$$A = \frac{E_{np}}{E_p}, \quad B = \frac{t_{np}}{t_p} \tag{2}$$

where k_{31} is the transverse coupling factor, E_{np} and E_p are Young's modulus of non-piezoelectric and piezoelectric parts, and t_{np} and t_p are the thickness of non-piezoelectric and piezoelectric parts, respectively. Assuming that the adopted substrate is SUS304, because it is far thicker than other non-piezoelectric layers of top and bottom electrodes, E_{np} and t_{np} are approximately equal to Young's modulus (197 GPa) and thickness of SUS304, respectively. E_p and k_{31} of AlN thin films are 330 GPa and 0.14 [16,28], respectively. Since k_{31} and A are constants, the calculated k_{eff} of the multilayered structure is a function of B, which is plotted in Fig. 3. The maximal k_{eff}^2 are achieved when the thickness ratio is 3.1. In other words, for 1 μm thick AlN thin film, k_{eff}^2 reaches the maximum when the thickness of SUS304 is 3.1 μm.

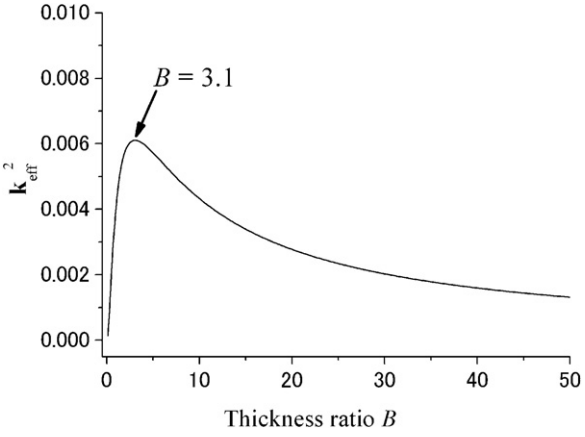

Fig. 3. Calcualted effective electromechanical coupling factor k_{eff} versus the thickness ratio B between the SUS304 substrate and AlN thin film.

It should be noted that in the practical fabrication of devices, the obtaining of the optimal thickness ratio may be difficult for some substrates due to the limit of the machining method and precision. Additional, too thin substrates may lead to serious bending or even breaking of devices if large residual stress exists in piezoelectric thin films.

3.3. Adjustment of resonant frequency of miniature piezoelectric generators

The frequency of vibration sources in environment is usually lower than 200 Hz. For optimizing the mechanical coupling, the resonant frequency of a piezoelectric generator should be adjusted to be equal or very near to the frequency of vibration sources. For a common cantilever with a uniform cross section, if it is assumed that only one end of the cantilever beam is fixed and the beam weight is uniform along the length, the initial resonance (f_0) can be written as below [29]:

$$f_0 = \frac{3.52}{2\pi}\sqrt{\frac{EIg}{vl^4}} = \frac{0.88}{\sqrt{3}\pi}\frac{t}{l^2}\sqrt{\frac{E}{\rho}} \tag{3}$$

where $I = wt^3/12$, $v = \rho gwt$, g is acceleration of gravity, and w, t, l, E and ρ are the width, thickness, length, Young's modulus and mass density of the cantilever, respectively. In a miniature generator with the multilayered structure including the piezoelectric layer, substrate, and electrodes, for simplifying the calculation, the effective Young's modulus (E_{eff}) and effective mass density (ρ_{eff}) are introduced according to the mixing rule:

$$E_{eff} = \frac{\sum_{i=1}^{n} E_i t_i}{\sum_{i=i}^{n} t_i} \tag{4}$$

$$\rho_{eff} = \frac{\sum_{i=1}^{n} \rho_i t_i}{\sum_{i=i}^{n} t_i} \tag{5}$$

where E_i, t_i, and ρ_i are Young's modulus, thickness and mass density of the ith layer, respectively. It can be seen that thinning the thickness of the substrate or increasing the length of the substrate are two effective approaches to reduce the resonant frequency of generators. For further reducing the resonant frequency of the piezoelectric generator, a proof mass is attached at the free end of the cantilever, and the resonant frequency (f') is formulated by [30]:

$$f' = f_0\sqrt{\frac{0.236m}{0.236m+M}} \tag{6}$$

where m is the mass of the cantilever, and M is the additional proof mass.

4. Fabrication and characterization of miniature AlN generators

In this study, SUS304 thin sheets were used as substrates of AlN thin films. AlN thin films were deposited in an electron cyclotron resonance (ECR) sputtering system in which plasma was produced by superimposing static magnetic field of 875 G and microwave of 2.45 GHz. The ECR deposition technology enables sputtering at very low pressure (10^{-3}–10^{-1} Pa) possible, therefore, it extremely results in lower contamination and smoother surface of the deposited films, in comparison with conventional sputtering techniques like RF or DC magnetron. The ECR sputtering chamber was pumped down to a base pressure of less than 1.6×10^{-5} Pa before Ar and N_2 gases were input. The details of the deposition process have been described in our previous reports [31,32].

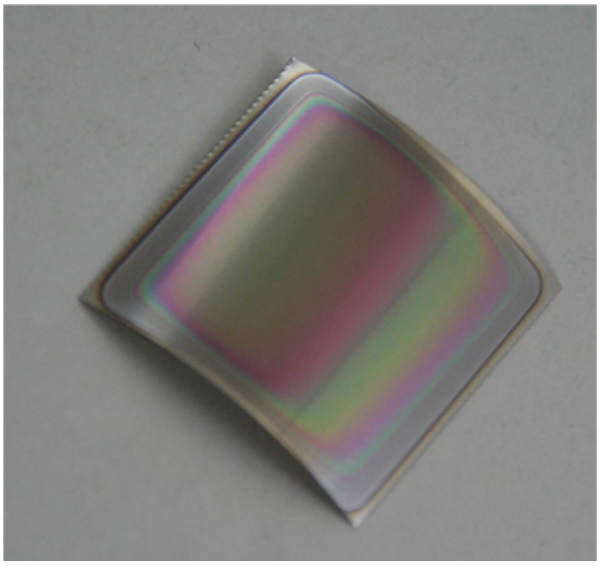

Fig. 4. Optical photo of an AlN thin film deposited on SUS304 with the ECR deposition.

Fig. 4 shows an optical photo of a 1.03 μm thick AlN thin film grown on a piece of 50 μm thick SUS304 (length × width: 20.0 mm × 20.0 mm). Residual stress in AlN bends the substrate convex upward, and thus it is compressive. The bending deflection at the center of the specimen is 2.3 mm, implying that residual stress is still very strong although the deposition parameters have been optimized [31]. The thickness ratio between SUS304 and AlN is 48.5, and it is far larger than the optimal thickness ratio of 3.1 at which the electromechanical coupling coefficient k_{31}^{G} theoretically reaches the maximal value according to Fig. 3. By considering that thinner SUS304 leads to more serious bending due to large residual stress, 50 μm thick SUS304 was adopted as substrates of AlN thin films for fabricating piezoelectric generators.

A layer of 200 nm thick Al top electrode was deposited on the surface of AlN/SUS with RF magnetron sputtering. The structure of Al/AlN/SUS was cut into small pieces, and each piece was fixed at one end with a clamper to form a cantilever. The free end of each cantilever was bonded with a copper proof mass. The top electrode and SUS substrate were, respectively, bonded with two metal wires to form a generator. Fig. 5(a) is the schematic illustration of an AlN generator, and Fig. 5(b) is the optical photo of the final prototype.

Table 5
Measured dimensions of the AlN/SUS generator.

l_1 (mm)	l_2 (mm)	l_b (mm)	l_m (mm)	t_p (μm)	t_s (μm)	t_m (mm)
2.1	5.4	6.2	4.1	1.03	50.0	5.1

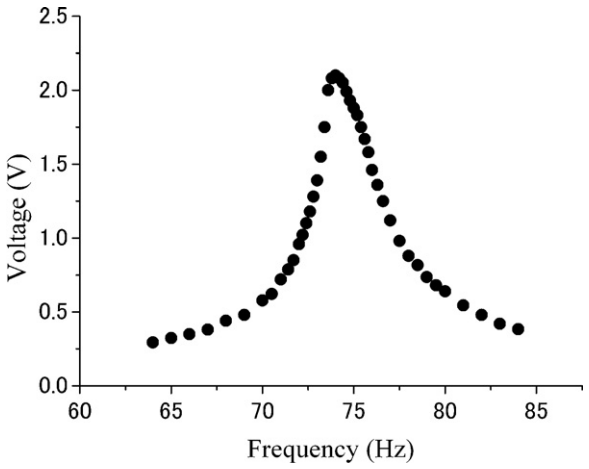

Fig. 6. Peak-to-peak voltage versus vibration frequency of an AlN generator vibrated at 0.2 g acceleration in open circuit.

The measured dimensions of the device are showed in Table 5. It can be seen that the ratio $G = l_1/l_2$ of AlN generators is 0.39, which is beneficial to obtain high transverse electromechanical coupling coefficient according to Fig. 2.

The vibration energy harvesting of AlN generators were investigated with a system including a vibrator, a function generator, a laser vibrometer and an oscilloscope. The devices were mounted on the vibrator that was controlled by the function generator. Vibration acceleration was monitored with the laser vibrometer. The voltage yielded from AlN generators was sinusoidal, and the peak-to-peak value (V_{p-p}) was recorded. The peak-to-peak voltage as a function of vibration frequency was displayed in Fig. 6 in which the device was vibrated at 0.2 g acceleration in open circuit. The peak-to-peak voltage reached the maximum of 2.10 V at resonant frequency of 74.1 Hz which was much lower than that of previously reported miniature generators.

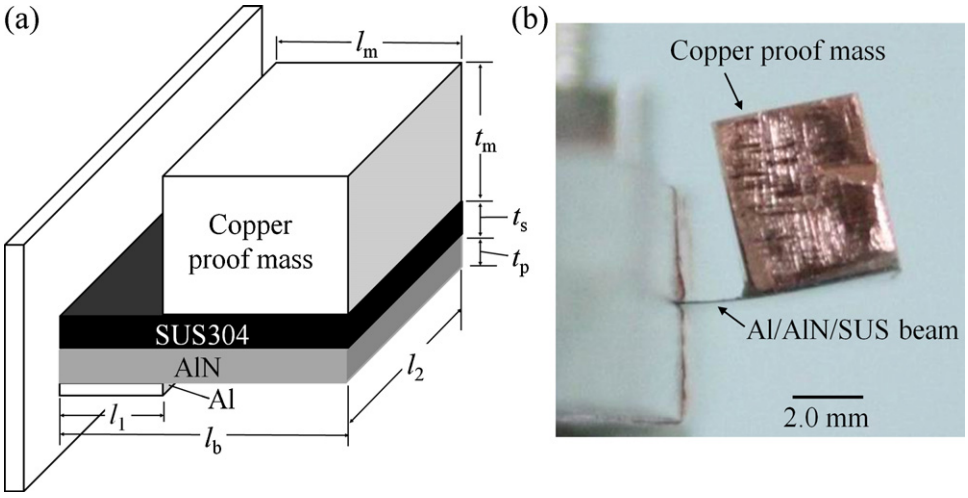

Fig. 5. (a) schematic illustration and (b) optical photo of a piezoelectric generator fabricated from AlN thin films that were deposited on SUS304 with the ECR deposition.

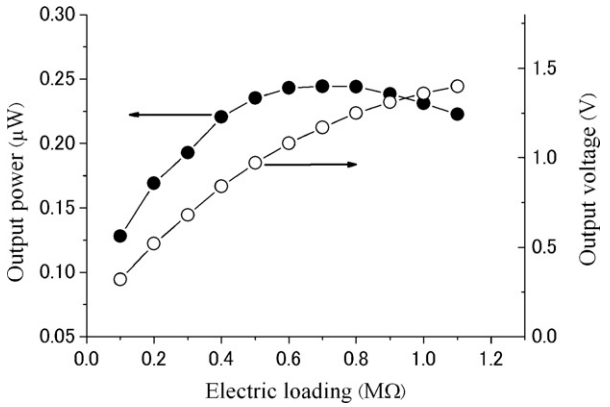

Fig. 7. Output voltage and power versus electric loading of an AlN generator vibrated at 0.2 g acceleration.

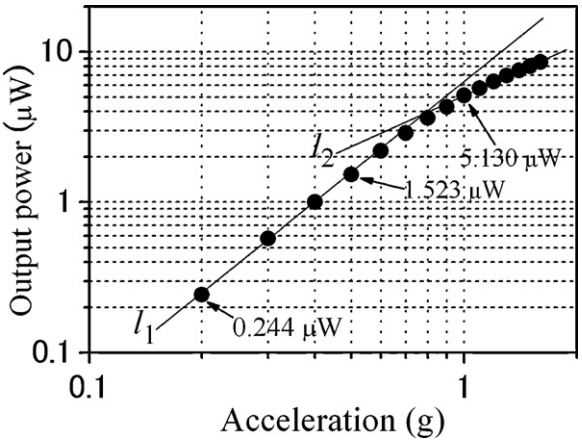

Fig. 8. Output power versus vibration acceleration of an AlN generator connected with 700 kΩ.

According to the peak-to-peak voltage, the output power can be calculated [6]:

$$P = \frac{V_{rms}^2}{R_L} = \frac{V_{p-p}^2}{8R_L} \tag{7}$$

where V_{rms} is the root-mean-square voltage and is equal to $\sqrt{2}V_{p-p}/4$, and R_L is the electric loading connected to generators. AlN generators were connected with a series of electric loading and vibrated at 0.2 g acceleration, and the output voltage and power were correspondingly demonstrated in Fig. 7. With the increase of electric loading, the output voltage monotonically increased; however, the output power firstly went up and then dropped. The optimal electric loading at which the output power reached the maximum of 0.244 μW was identified to be 0.7 MΩ. The optimal electric loading R_{opt} can also be calculated according to the following equation [33,34]:

$$R_{opt} = \frac{1}{2\pi fc}\sqrt{\frac{1}{1+Q^2K^4}} \tag{8}$$

where f is the vibration frequency and C is the electric capacity of the piezoelectric generator. Assuming that dielectric constant of AlN thin films = 10 and $Q^2K^4 \ll 1$, the calculated value of the optimal loading is 0.772 MΩ, which agrees with the experimental value.

Fig. 8 shows the double logarithmic plot of output power verse vibration acceleration. As the vibration acceleration increased, the output power rapidly increased. At 0.5 g acceleration, the output power was 1.523 μW and the resonant frequency was shifted to 71.6 Hz. At 1 g acceleration, the output power was 5.130 μW and the resonant frequency was moved to 69.8 Hz. When the acceleration ascended to 1.6 g, the power reached 8.555 μW. The slope of l_1 is 1.94, revealing that output power at low acceleration increased in an approximately quadratic relationship with the acceleration. This result is consistent with the model of a velocity damped oscillator that was assumed before [35]. The slope of l_2 is 0.99, which may be attributed to stronger damping at violent vibration and smaller piezoelectric constant under larger stress.

A comparison of AlN generators with two different aspect ratios is given in Table 6. The structures of AlN/SUS in these two kinds of generators are the same. Although the beam area of the AlN generator in this study is a little smaller than that of the one reported in our previous report [32], the output power of the former is almost twice that of the latter. This can be contributed to the smaller aspect ratio in the former. Another comparison of our devices with some recently reported PZT and AlN miniature generators is demonstrated in Table 7. It shows that the resonant frequency of our

Table 6
Comparison of AlN/SUS generators with two different aspect ratios.

	Aspect ratio	Beam: length × width (mm × mm)	Mass: length × width × height (mm × mm × mm)	Power at 1 g (μW)	Resonant frequency (Hz)
In this study	0.39	2.0 × 5.4	4.1 × 5.4 × 5.1	5.130	69.8
In previous study [32]	2.71	6.5 × 2.4	4.6 × 7.5 × 1.5	2.614	55.2

Table 7
Comparison of various PZT and AlN miniature generators.

Author	Device	Effective volume (mm^3)	Power (μW)	Acceleration (g)	Resonant frequency (Hz)
Jeon et al. [5]	d_{31} PZT cantilever	Unclear	1.01	10.6	13.9k
Fang et al. [6]	d_{31} PZT cantilever	0.199	2.16	1.0	608
Shen et al. [7]	d_{31} PZT cantilever	0.652	2.15	2.0	462
Lee et al. [13]	d_{33} PZT cantilever	0.424	2.10	2	256
Park et al. [14]	d_{33} PZT cantilever	0.990	1.1	0.39	528
Marzencki et al. [8]	d_{31} AlN cantilever	>0.504	0.8	2	1495
Elfrink et al. [9]	d_{31} AlN cantilever	>7.725	60	2.0	572
Zhang et al. [31]	d_{31} AlN cantilever	0.251	1.42	1.0	1042.6
In this study	d_{31} AlN cantilever	Cantilever: 1.647 Proof mass: 112.9	5.130	1.0	69.8
In this study	d_{31} AlN cantilever	Cantilever: 1.647 Proof mass: 112.9	8.555	1.6	69.1

devices is far lower than that of the reported generators. The volume of the cantilever beam in our study is in the approximate level with that of the listed devices, but the volume of the proof mass in ours is much larger than that of other generators. The large size of the proof mass is due to: thick SUS substrates in our device need a heavy proof mass for reducing the resonant frequency. It should be noted that if residual stress in AlN thin films can be markedly suppressed to a low enough level, thin SUS substrates of with the thickness of less than 10 μm can be used for fabricating generators without serious beam bending. In this case, the size of the proof mass can be significantly minimized. In the near future, this work will be carried out.

5. Conclusions

Both material selection and device configuration design were analyzed for fabricating miniature piezoelectric generators. For obtaining generators with low frequency and high mechanical strength, 50 μm thick SUS is chosen as the substrate of piezoelectric thin films. For improving the energy conversion efficiency, the cantilever configuration including the aspect ratio and the thickness ratio were theoretically optimized by the consideration of enhancing the effective electromechanical coupling coefficient. For the structure of AlN/SUS, the preferred aspect ratio is less than 0.4, and the optimal thickness ratio is 3.1.

With the ECR sputtering deposition, 1.03 μm thick AlN thin films were deposited on 50 μm thick SUS304. Millimeter-scale generators were fabricated and their vibration energy harvesting was characterized. Output power and resonant frequency of the devices were, respectively, 5.13 μW and 69.8 Hz when they were vibrated at 1 g acceleration and connected with 0.7 MΩ electric loading. Energy conversion efficiency of generators in the present study was evidently higher than that of generators in our previous report [32], which was contributed more suitable aspect ratio in this study.

References

[1] S.R. Anton, H.A. Sodano, Smart Mater. Struct. 16 (2007) R1–R21.
[2] K.A. Cook-Chennault, N. Thambi, A.M. Sastry, Smart Mater. Struct. 17 (2008) 1–33.
[3] N.S. Hudak, G.G. Amatucci, J. Appl. Phys. 103 (2008) 101301.
[4] A. Khaligh, P. Zeng, C. Zheng, IEEE Trans. Ind. Electron. 57 (2010) 850–860.
[5] Y.B. Jeon, R. Sood, J.H. Jeong, S.G. Kim, Sens. Actuators A 122 (2005) 16–22.
[6] H.B. Fang, J.Q. Liu, Z.Y. Xu, L. Dong, L. Wang, D. Chen, B.C. Cai, Y. Liu, Microelectron. J. 37 (2005) 1280–1284.
[7] D. Shen, J.H. Park, J. Ajisaria, S.Y. Choe, H.C. Wikle, D.J. Kim, J. Micromech. Microeng. 18 (2008) 055017.
[8] M. Marzencki, Y. Ammar, S. Basrour, Sens. Actuators A 145–146 (2008) 363–370.
[9] R. Elfrink, T.M. Kamel, M. Goedbloed, S. Matova, D. Hohlfeld, Y.V. Andel, R.V. Schaijk, J. Micromech. Microeng. 19 (2009) 094005.
[10] Q.M. Wang, X.H. Du, B. Xu, L.E. Cross, IEEE Trans. Ultrason. Freq. Contr. 46 (1999) 638–646.
[11] M.F. Aimi, M.P. Rao, N.C. Macdonald, A.S. Zuruzi, D.P. Bothman, Nat. Mater. 3 (2004) 103–105.
[12] E.R. Parker, M.P. Rao, K.L. Turner, C.D. Meinhart, N.C. Macdonal, J. Microelectromech. Syst. 16 (2007) 289–294.
[13] B.S. Lee, S.C. Lin, W.J. Wu, X.Y. Wang, P.Z. Chang, C.K. Lee, J. Micromech. Microeng. 19 (2009) 065014.
[14] J.C. Park, J.Y. Park, Y.P. Lee, J. Microelectromech. Syst. 19 (2010) 1215.
[15] N. Ledermann, P. Muralt, J. Baborowski, S. Gentil, K. Mukati, M. Cantoni, A. Seifert, N. Setter, Sens. Actuators A 105 (2003) 162–170.
[16] K. Tsubouchi, N. Mikoshiba, IEEE Trans. Son. Ultrason. 32 (1985) 634–644.
[17] I.B. Kobiakov, Solid State Commun. 35 (1980) 305–310.
[18] S. Trolier-Mckinstry, P. Muralt, J. Electroceram. 12 (2004) 7–17.
[19] S. Baik, S.M. Lee, J. Mater. Sci. 29 (1994) 6115–6122.
[20] R. Fu, T.Y. Zhang, J. Am. Ceram. Soc. 81 (1998) 1058–1060.
[21] H. Wang, H.T. Lin, A.A. Wereszcak, J. Am. Ceram. Soc. 93 (2010) 2843–2849.
[22] K.M. Taylor, C. Lenie, J. Electrochem. Soc. 107 (1960) 308–314.
[23] http://accuratus.com/alumni.html.
[24] B. Balzer, M. Hagemeister, P. Kocher, L. Gauckler, J. Am. Ceram. Soc. 87 (2004) 1932–1938.
[25] ANSI/IEEE, Standard on Piezoelectrics, 1987.
[26] J. Kim, M. Kim, K. Ha, W. Cao, Jpn. J. Appl. Phys. 46 (2007) 4459–4461.
[27] C. Chen, R. Zhang, Z. Wang, W. Cao, J. Appl. Phys. 105 (2009) 064104.
[28] A.F. Wright, J. Appl. Phys. 82 (1997) 2833–2839.
[29] C. Liu, Foundations of MEMS, Pearson Prentice Hall, New York, 2006.
[30] J. Merhaut, Theory of Electroacoustics, McGraw-Hill, New York, 1981.
[31] J.Y. Zhang, Z.P. Cao, H. Kuwano, Jpn. J. Appl. Phys. 50 (2011) 09ND18.
[32] Z.P. Cao, J.Y. Zhang, H. Kuwano, Power MEMS—The 11th Int. Workshop on Micro and Nanotechnology for Power Generation and Energy Conversion Applications, Seoul, Korea, 2011.
[33] K. Morimoto, I. Kanno, K. Wasa, H. Kotera, Sens. Actuators A 163 (2010) 428–432.
[34] T.H. Ng, W.H. Liao, J. Intell. Mater. Syst. Struct. 16 (2005) 785–797.
[35] S. Roundry, R.K. Wright, J.M. Rabaey, Energy Scavenging for Wireless Sensor Networks, Kluwer, Dordrecht, 2003.